LETTER • OPEN ACCESS

Spaceborne evidence for significant anthropogenic VOC trends in Asian cities over 2005–2019

To cite this article: M Bauwens *et al* 2022 *Environ. Res. Lett.* **17** 015008

View the article online for updates and enhancements.

ENVIRONMENTAL RESEARCH
LETTERS

LETTER

Spaceborne evidence for significant anthropogenic VOC trends in Asian cities over 2005–2019

M Bauwens[*], B Verreyken[1] , T Stavrakou[*] , J-F Müller and I De Smedt

Royal Belgian Institute for Space Aeronomy (BIRA-IASB), Brussels, Belgium
[1] Present address: NOAA Earth System Research Laboratories, Boulder, CO 80305, United States of America.
[*] Authors to whom any correspondence should be addressed.

E-mail: trissevgeni.stavrakou@aeronomie.be

Abstract

Trends of formaldehyde (HCHO) linked to anthropogenic activity over large cities located in the Asian continent are calculated for the period 2005–2019 using the Quality Assurance for Essential Climate Variables dataset from the Ozone Monitoring Instrument aboard the Aura satellite. Contributions due to anthropogenic emissions are isolated by applying a correction based on near-surface temperature in order to account for interference from local biogenic emissions. Strong positive trends are derived over the Middle East and the Indian subcontinent (up to 3.6% yr^{-1} and 2.4% yr^{-1} respectively) where regulations of anthropogenic non-methane volatile organic compound (NMVOC) emissions are currently limited. Weaker trends are observed over cities located in China, where the air pollution action plan (2013) may have mitigated NMVOC trends early on, but targeted legislature concerning VOC emissions was only recently introduced. HCHO trends for cities located in South and Equatorial Asia are mostly not significant or very uncertain. Cities located in Taiwan and Japan (regions in Asia where legislation has been in place since the early 2000s) display mostly negative trends.

1. Introduction

Anthropogenic non-methane volatile organic compounds (AVOCs) are key atmospheric constituents affecting air quality and the climate through their role in the formation of ozone and secondary organic aerosols. Emissions of AVOCs are significant in urban and industrialized areas and their major sources include fossil fuel and biofuel production and use, industrial processes, solvent use, and road transport (Ehhalt *et al* 2001). Bottom-up estimates indicate an increase of ca. 40% of the global AVOC emissions between 1970 and 2012, with Asia being the largest contributor (Huang *et al* 2017). However, regional and global AVOC emission inventories have large uncertainties, due to the strong spatiotemporal variability and high variety of their sources, and to the relative lack of accurate information, particularly in Asia. In comparison, NO$_x$ emissions and trends are relatively better quantified, to a large extent thanks to the monitoring of tropospheric NO$_2$ columns from satellites (Duncan *et al* 2016). Due to

the harmful effects of AVOCs on human health and the environment, those compounds are increasingly attracting the attention of policy makers (He *et al* 2019, Zhao *et al* 2020). This has led to a gradual tightening of VOC emission regulations, especially in the US, Europe and Japan. However, these regulations are very diverse across Asian countries. Whereas Japan and Taiwan promulgated AVOC emission controls since the early 2000s (Botta and Yamasaki 2020, EPA-Taiwan (Environmental Protection Administration) 2020), China and Korea formulated VOC emission regulations only recently (Tsai 2016, China VOCs Management 2021). In India, clean air action plans for cities are currently developed (Bhave and Kulkarni 2015, Ganguly *et al* 2020) but no VOC regulations have been adopted so far, except for benzene (Sekar *et al* 2019). In the Middle East and central Asian countries, regulations are limited and emission standards vary among countries (Sekar *et al* 2019). The success of VOC regulations largely depends on monitoring, assessing and controlling strategies, which are country-dependent

(San *et al* 2018). In addition to regulations, factors like population growth, economical and industrial development, and new technologies, strongly influence the AVOC emissions and their evolution. The estimation of emissions and their trends becomes therefore very challenging.

A detailed comparison between available bottom-up and top-down inventories (Elguindi *et al* 2020) showed a general agreement that AVOC emissions from China are increasing, although there are important discrepancies among the reported trends. Similarly, the REASv3 bottom-up inventory over Asia (Kurokawa and Ohara 2020) reported that most inventories indicated increasing trends over China after the early 2000s. Most inventories showed continuously increasing AVOC emissions over India while for Japan, emissions have decreased in recent decades. Despite these similarities in AVOC emissions across different inventories, large differences are also found.

Spaceborne observations of formaldehyde (HCHO), a high yield intermediate in the oxidation of the majority of VOCs released into the atmosphere, have been widely used to constrain the VOC emissions from biogenic and biomass burning origin at global and regional scale (Millet *et al* 2008, Barkley *et al* 2013, Bauwens *et al* 2016). However, the application of inverse methods to derive AVOC emissions is challenging due to the generally weak HCHO signal due to anthropogenic sources relative to the biogenic and pyrogenic emissions. A few studies focused on heavily polluted regions where AVOCs are expected to have a strong contribution to the HCHO signal. Barkley *et al* (2017) reported significant positive HCHO trends in anthropogenic point sources in the Middle East over 2005–2014 using observations from the Ozone Monitoring Instrument (OMI, Levelt *et al* 2006). OMI HCHO observations were used to detect urban and industrial plumes in Nigeria (Marais *et al* 2014), eastern Texas (Zhu *et al* 2017), and eastern China (Shen *et al* 2019), and as constraints in inversion studies over China (Stavrakou *et al* 2017, Cao *et al* 2018) and India (Chaliyakunnel *et al* 2019).

Using spaceborne observations to monitor the efficacy of environmental regulations for controlling VOCs is hampered by the masking effect of other VOCs sources—primarily terrestrial vegetation (Palmer *et al* 2006, Stavrakou *et al* 2009). Nevertheless, this study shows that emission trends can be accurately monitored based on HCHO column data retrieved from the OMI satellite instrument over 15 years, from 2005 to 2019 around large cities in Asia. Since the interannual variability of HCHO columns is affected by climate variability (Palmer *et al* 2006), primarily due to the dependence of biogenic VOC (BVOC) emissions on temperature and solar radiation, and because this contribution might be significant even around large cities, we subtract the contribution of climate variability to the long-term

observed HCHO trends using the temperature correction method suggested in Shen *et al* (2019). This study focuses for the first time on the detection of AVOC trends over a large number of Asian cities using satellite data, and aims to complement the current body of literature on AVOC emissions in Asia (e.g. Zheng *et al* 2018, Kurokawa and Ohara 2020).

The satellite-based urban HCHO trends are discussed and compared to the estimated AVOC emission trends in bottom-up inventories and to the respective OMI NO_2 trends calculated over the same cities. VOC and NO_x are the key ingredients in the formation of tropospheric ozone (Calvert *et al* 2015), of which abundances have been generally increasing over East and South Asia in the last decades (Nelson *et al* 2021). Although road transport and other sectors contribute significantly to both AVOC and NO_x emissions, the AVOC/NO_x emission ratio is sector-dependent and some of the major sources of NO_x and AVOC (power generation and solvent use, respectively) are markedly different (Li *et al* 2017). Moreover, emission controls might affect AVOC and NO_x differently, resulting in important differences regarding their temporal evolution.

2. Methodology

We use HCHO and NO_2 data retrieved from the OMI nadir-viewing instrument, both developed in the framework of the EU FP7 project Quality Assurance for Essential Climate Variables (Boersma *et al* 2017, De Smedt *et al* 2018) for the period 2005 to the present. OMI follows a sun-synchronous, low-Earth orbit with an Equator local overpass time of ca. 13:45 and has a resolution of 13×24 km^2 at nadir (Levelt *et al* 2006). The HCHO data set is based on the differential optical absorption spectroscopy algorithm described in De Smedt *et al* (2018). Here we use observations with cloud fractions lower than 20% in order to minimize potential effects from clouds. The NO_2 data set is based on revised spectral fitting features, accounting for improved absorption cross sections, instrument calibration, and surface effects (Boersma *et al* 2018, Zara *et al* 2018). The data are processed according to the data quality recommendations with a cloud filter set at 40%. For monthly mean OMI HCHO and NO_2 column data, the detection limit is estimated at 2.5×10^{15} molec cm^{-2} (De Smedt *et al* 2021) and at 1.0×10^{15} molec cm^{-2} (Compernolle *et al* 2020), respectively. The satellite products were recently validated against MAX-DOAS (Multiple AXis-Differential Optical Absorption Spectroscopy) ground-based observations (Wang *et al* 2019, Compernolle *et al* 2020, De Smedt *et al* 2021).

We focus on the summer months, from May to September, as the prompt oxidation of VOCs in this season provides a stronger HCHO signal compared to winter, where HCHO levels are lower due to the weak photochemical source of HCHO. Furthermore,

the retrieval errors for both HCHO and NO_2 are lower in summer, and are estimated to 40%–60%, and 20%–55%, respectively, for the cities considered here.

We selected cities with a population of over 500 000 inhabitants for China and India, or over 300 000 inhabitants for other Asian countries based on the Geonames geographical database (www.geonames.org, last access: 10 November 2021). We select cities where (a) the AVOC emission flux based on the EDGARv4.3.3 emission inventory (Huang *et al* 2017) over May–September is higher than a threshold value, taken equal to 6 g m^{-2}, and (b) the ratio of anthropogenic to BVOC emissions is higher than 3. Those thresholds were chosen to ensure that the AVOC emission of the city is sufficiently important and is significantly larger than the local biogenic emissions. The biogenic emissions (sum of isoprene, monoterpenes, and methanol) are obtained from the MEGAN-MOHYCAN model (Müller *et al* 2008, Stavrakou *et al* 2018). The above criteria lead to a total of 133 cities in 31 Asian countries for further analysis (listed in table S1 (available online at stacks.iop.org/ERL/17/015008/mmedia)). To generate the OMI HCHO time series for these cities, all observations in an overpass area of a 30 km radius around the city centers are averaged per month. The monthly mean is not considered when less than five observations are available in a given month. A smaller radius (e.g. 15–20 km) would strongly reduce the amount of available observations per month and would lead to noisier monthly averages. Moreover, in order to remove potential interferences from fire emissions, we exclude specific regions and months with fire episodes. Such regions are the North China Plain (32°–40° N, 112.5°–120° E) in June and the Indo-Gangetic Plain (26°–34° N, 70°–86° E) in May, due to agricultural residue burning (Liu *et al* 2015, Stavrakou *et al* 2016, Bray *et al* 2019), and the entire equatorial band (10° S–10° N) in September, which coincides with the beginning of the fire season.

To take out the effects of climate variations on the interannual variability of the HCHO columns, we apply a temperature-correction method on the monthly HCHO columns following the approach of Zhu *et al* (2017) and Shen *et al* (2019). To this purpose, the monthly mean HCHO columns for the selected cities between May and September over 2005–2019 are regressed onto the monthly averaged daily maximum surface air temperature, obtained by the ECMWF ERA5 (European Centre for Medium-Range Weather Forecasts Reanalysis Fifth Generation) reanalysis fields (Hesbach *et al* 2020). The fitted temperature dependency is then subtracted from the original time series. Trends are calculated using a linear regression of the annual May-to-September mean corrected columns and are considered significant when their absolute value exceeds their $1 - \sigma$ uncertainty.

As for the HCHO columns, we use OMI NO_2 data within 30 km of the city centers of the selected cities (table S1) between May and September for all years of the 2005–2019 period and derive urban NO_2 trends using a linear regression method.

3. Results

The HCHO trends for the selected cities are illustrated in figure 1, whereas the trends detected as being significant are detailed in figure 2. Of the 133 studied cities, significant trends are found for 77 cities (table S1). Positive HCHO trends are found for most urban areas, and clear regional patterns can be identified.

The trends observed over China are relatively weak and mostly positive, typically between $+0.5\%$ yr^{-1} and $+1.5\%$ yr^{-1} and negative in only two cities, namely Dongguan in the Pearl River Delta and Chengdu in western China. In the Indian subcontinent, strong positive trends are observed, estimated on average at 1.4% yr^{-1} and ranging between $0.7 \pm 0.5\%$ yr^{-1} (Karachi) and $2.4 \pm 0.7\%$ yr^{-1} (Peshawar). Positive trends are also found over the Middle East and central Asia reaching up to $3.6 \pm 0.6\%$ yr^{-1} (Karaj, Iran). No significant trends were observed over Istanbul and Ankara in Turkey.

Trends are often not significant in southeast and equatorial Asian countries, except over Bandung (Indonesia), Cebu city (Philippines) and Hanoi (Vietnam), with trends exceeding 2% yr^{-1}.

Significant negative trends are found in Japan, estimated on average at -1.5% yr^{-1} for all considered cities. In Taiwan, the HCHO trends are also mostly negative, except in Taichung.

Figure 3 compares the temporal evolution of (temperature-corrected) HCHO columns and NO_2 columns, relative to 2005, for a selection of 25 cities. The 2005–2019 NO_2 trends for all 133 cities are shown figure S1. The Chinese megacities generally exhibit strong reductions in NO_2 levels between 2005 and 2019 (up to -60%). For most cities, NO_2 columns increase in the first part of the period (2005–2010/2014) and decline afterwards. Over large industrial centers such as Shanghai, Guangzhou and Shenzhen, the NO_2 decline started already after 2007. This is in contrast with the HCHO column evolution in Chinese cities, with generally either positive (figure 2) or negligible trends (e.g. Shanghai and Guangzhou, figures 3(c) and (d)).

A notable exception is Chengdu, where the HCHO trend is negative ($-1.2 \pm 0.6\%$ yr^{-1}). The net reduction over Chengdu between 2005 and 2019 is 20% for HCHO and 60% for NO_2.

Over large Indian and Pakistani cities (figures 3(k)–(o) and (w)), NO_2 columns display only small trends between 2005 and 2019, and declines are even found after 2013 in Delhi and Chennai, whereas HCHO columns increased over most cities. Over
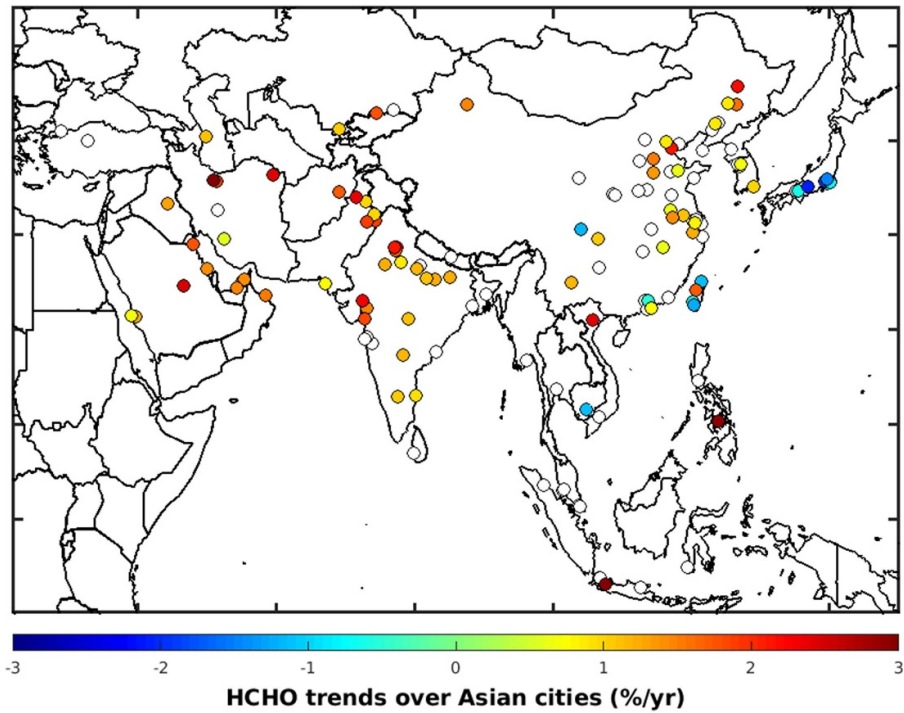
Figure 1. Temperature-corrected HCHO trends (in % yr^{-1}) over the Asian cities considered in this study (133). Colored circles denote cities for which significant trends are detected (77), white circles denote cities with no significant trends (56).
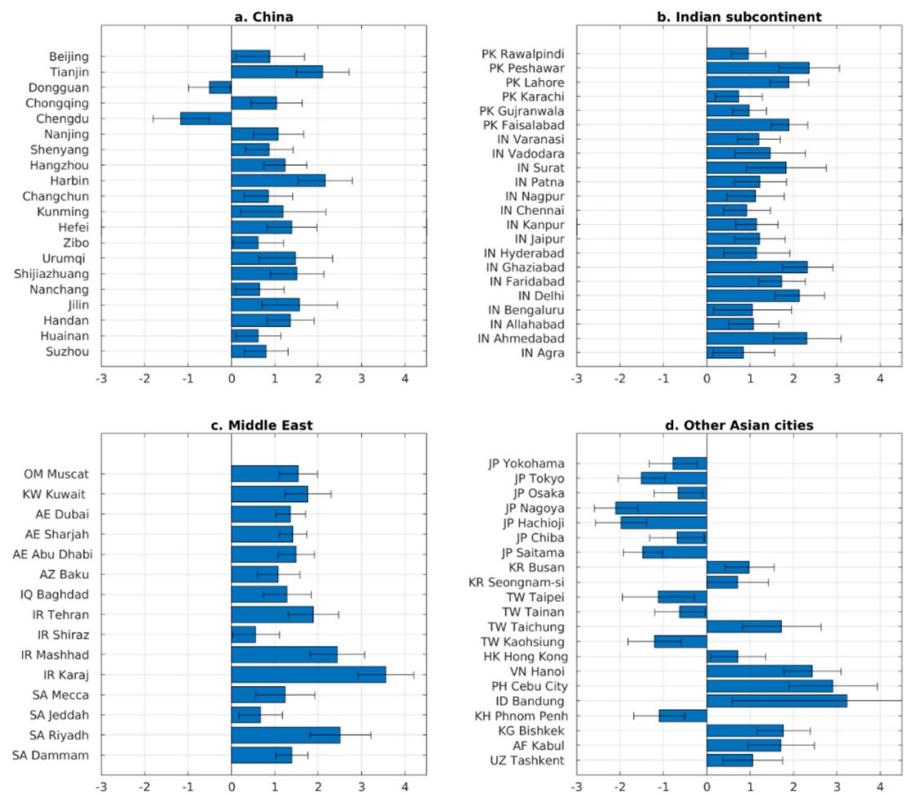

Figure 2. HCHO trends expressed in % yr^{-1} for large cities in China (a), the Indian subcontinent (b), the Middle East (c) and other Asian countries (d). Error bars indicate the $1 - \sigma$ uncertainty on the obtained trends. The country code and the city names are provided in (b)–(d). Cities for which the trend is not significant are not shown.
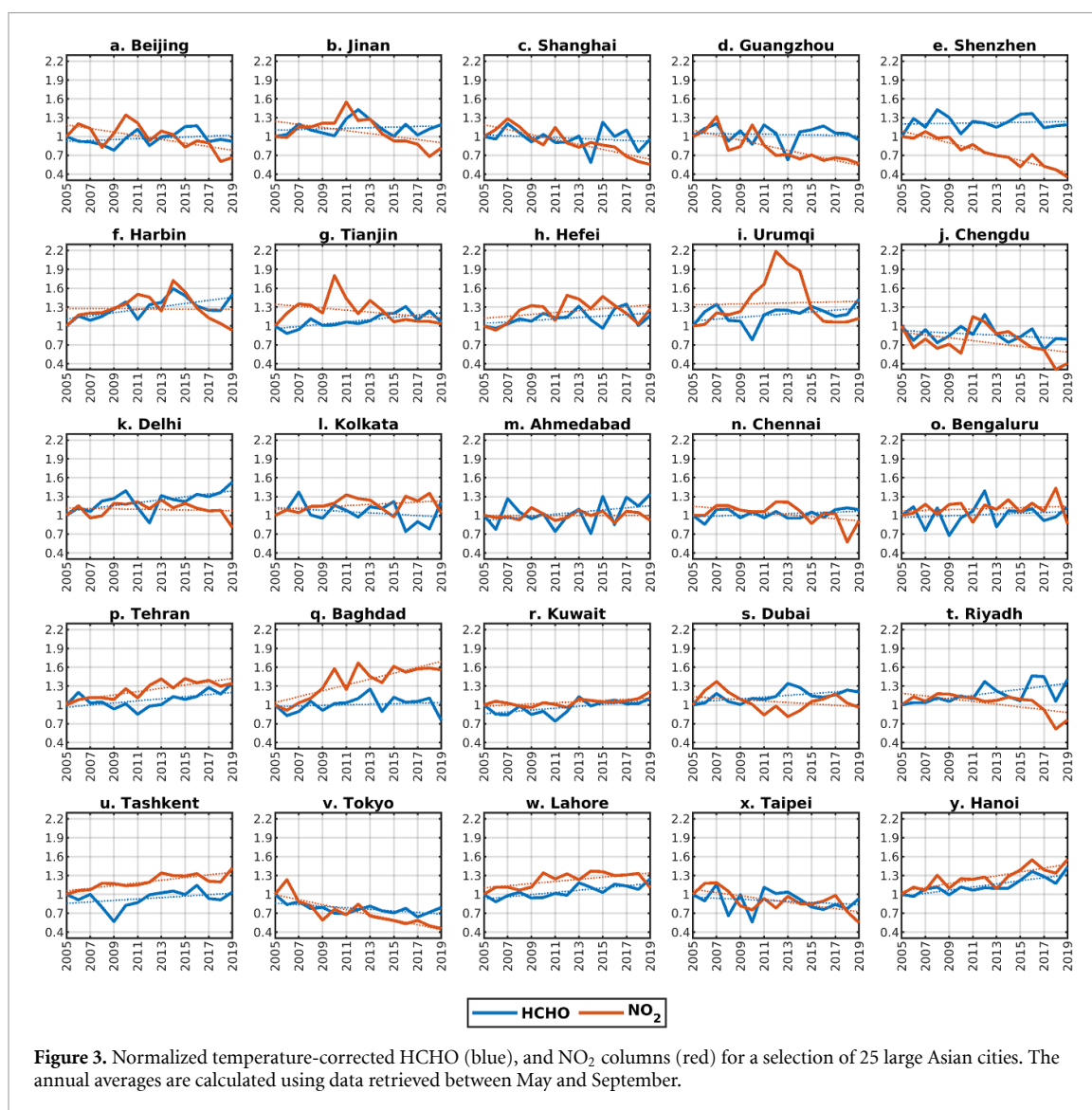
Figure 3. Normalized temperature-corrected HCHO (blue), and NO$_2$ columns (red) for a selection of 25 large Asian cities. The annual averages are calculated using data retrieved between May and September.
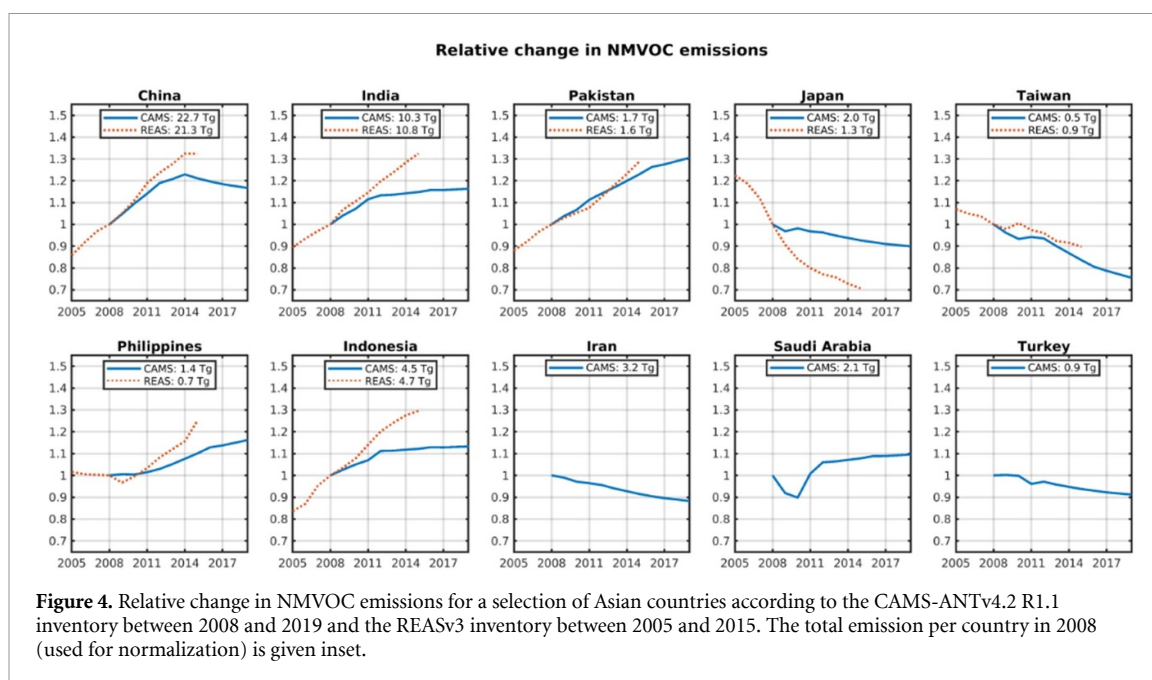
the Arabian Peninsula, NO$_2$ decreases while HCHO increases, by up to +37% in Riyadh between 2005 and 2019. In Iraq, Iran, Uzbekistan (Tashkent) and Vietnam (Hanoi) significant positive trends in both HCHO and NO$_2$ columns are found. In Tokyo and Taipei, we observe simultaneously negative changes in HCHO (−22% and −16%, respectively) and NO$_2$ columns (−56% and −28%) between 2005 and 2019.

4. Discussion

The HCHO trends over China presented above for 2005–2019 are consistent with the predominantly positive anthropogenic trends derived over China between 2005 and 2016 by Shen *et al* (2019) (up to +2.2% yr^{-1}). In line with their analysis, stronger trends are observed over the Yangtze River Delta and the North China Plain. The important reduction in HCHO and NO$_2$ observed over Chengdu and in the Pearl River Delta (Dongguan) shows that local efforts to counteract pollution are also evident from space observations. In those regions, the implementation

of air pollution control policies has shown improvements in recent years (Gao *et al* 2019, 2021), whereas AVOCs have become one of key pollution control targets (Gao *et al* 2019). In August 2017, an Air Pollution Prevention campaign, addressing AVOC emissions, was performed in Chengdu leading to immediate AVOC emission reduction of 25% (Tan *et al* 2020), likely contributing to the HCHO column decline observed over Chengdu in 2017 (figure 3).

In India and Pakistan, the strong positive HCHO trends are in line with the strong economic growth and near-absence of VOC emission regulations in the fast growing cities of the Indian subcontinent (Ganguly *et al* 2020). The strong trends observed over Delhi (+2.1 ± 0.6% yr^{-1}) and Kanpur (+1.2 ± 0.5% yr^{-1}) are consistent with the independent satellite-based analysis of Vohra *et al* (2020), which derived similar HCHO trends (+1.9% yr^{-1} for Delhi, +1.0% yr^{-1} for Kanpur). Note that their work corrected for the background contribution of longer-lived VOCs but not for biogenic contributions.

Figure 4. Relative change in NMVOC emissions for a selection of Asian countries according to the CAMS-ANTv4.2 R1.1 inventory between 2008 and 2019 and the REASv3 inventory between 2005 and 2015. The total emission per country in 2008 (used for normalization) is given inset.

Furthermore, our results for the Middle East are qualitatively in line with Barkley *et al* (2017), who also deduced strong HCHO trends in urban locations over 2005–2014 using OMI observations. In agreement with our analysis, they reported significant HCHO trends along the Persian Gulf coast, between 1% and 3% yr^{-1}, and in Riyadh (1.97% yr^{-1} vs 2.5 ± 0.7% yr^{-1} in this study). In Bagdad, they found an increased NO$_2$ trend, not seen in HCHO data, which was attributed to increased NO$_2$ emission from the Daura refinery located close to the city (Barkley *et al* 2017).

In south and equatorial Asia, the HCHO trends are more uncertain and are significant in only 4 out of the 16 cities considered. This can be explained by the comparably lower HCHO levels and larger associated uncertainties in these regions and by the strict cloud filter used (20%) which removes a large fraction of the data. In addition, uncertainties in the biogenic emissions around cities of equatorial Asia might cause larger errors in the derived trends. In Cebu and Bandung, although the trends are significant, their high uncertainty reflects the strong interannual column variation in these cities (+2.9 ± 1.0% yr^{-1} and +3.2 ± 2.6% yr^{-1}).

The observed declining trend in Phnom Penh (−1.1 ± 0.6% yr^{-1}) is at odds with the increase of AVOC emissions reported in San *et al* (2018), which is based on economic activity and industrial data. The discrepancy could be related to the large deforestation rates observed in the humid primary forests located within a radius of 150 km around the city (Hansen *et al* 2013). When considering the effects of land use changes on isoprene fluxes (Opacka *et al* 2021), the isoprene emissions around Phnom Penh over 2005–2019 are found to decline by about 1% yr^{-1}, suggesting that the trend in HCHO columns might

be partly due to forest loss in the regions surrounding Phnom Penh.

The significant positive HCHO trend in Hanoi (+2.4 ± 0.7% yr^{-1}), one of the fastest growing cities of Asia, is well supported by the increase of 36% in AVOC emissions suggested by the CAMS-ANTv4.2 R1.1 (Granier *et al* 2019) bottom-up inventory between 2008 and 2019. Figure S1 shows relatively weak NO$_2$ trends over most cities in south and equatorial Asia with the exception of the strong positive trends observed over the fast-developing cities of northern Vietnam.

Finally, the negative HCHO trends in Japan and Taiwan reflect the VOC emission regulations that have been promulgated earlier on, compared to other Asian countries, in combination with a weaker population growth. Over Japan, where the population growth is <+0.5% yr^{-1} for all cities under consideration (United Nations Department of Economic and Social Affairs 2021), satellite observations are in line with ground-based observations of Wakamatsu *et al* (2013), which showed continuously declining AVOC concentrations since 1970. It was estimated that VOC emissions from stationary sources in Japan were reduced by 42% between 2000 and 2009 (Wakamatsu *et al* 2013). In Taiwan, we find negative HCHO trends in all cities except for Taichung. This may reflect the stronger population growth in Taichung (+1.8% yr^{-1}), whereas the population growth for the other Taiwanese cities is much smaller (<+1% yr^{-1}, United Nations Department of Economic and Social Affairs 2021).

The observed HCHO trends agree qualitatively with the AVOC emission trends estimated by the CAMS-ANTv4.2 R1.1 (Granier *et al* 2019) and the REASv3 (Kurokawa and Ohara 2020) bottom-up inventories (figure 4). Both datasets

suggest increasing emissions in most Asian countries and declining emissions in Japan and Taiwan. While the increasing AVOC trends in most Asian countries are consistent with the trends in figure 1, the magnitude of the trends is not always consistent with OMI observations. Over Iran, the continuous AVOC emission decrease according to CAMS (Copernicus Atmosphere Monitoring Service) is not supported by OMI, in particular in Tehran where HCHO is found to increase rapidly after 2011.

More pronounced negative HCHO trends are derived over Japan than over Taiwan, in better consistency with the emission estimates from REASv3 than those from CAMS. Additionally, our analysis suggests similar HCHO trends in India and Pakistan while those over Chinese cities are much weaker. REASv3, however, suggests similar AVOC emission trends for all three countries and CAMS estimates similar increases in AVOC emissions for India and China, but stronger trends over Pakistan (figure 4). Note however that the REASv3 inventory does not extend after 2015, when AVOC emissions over China were at their maximum according to CAMS, in good consistency with the observed evolution of HCHO columns (figure 3).

The observed differences between trends in HCHO and NO_2 are also present in the AVOC and NO_x emissions from the CANT-ANTv4.2 R1.1 inventory (figure S2). This is especially true for China, where the Air Pollution Prevention and Control Action Plan has been introduced in 2013, but AVOCs were not specifically targeted until 2018 (China VOCs Management 2021). The differences in NO_2 and HCHO trends originate from the fact that they are not emitted by the same anthropogenic activities. For instance, solvents significantly contribute to the total AVOC emissions while they account for only a small fraction of NO_x emissions (figure S3). In contrast, the energy sector strongly contributes to the NO_x emissions but not to AVOCs. The discrepancies between AVOC emissions and NO_x are especially pronounced in China where industrial sources and solvent use were the main drivers of the rise of AVOC concentrations while reduced emissions from residential biofuel use and on-road vehicle exhaust (which account for a large fraction of NO_x emissions) mitigated the rapid growth rates in the last decade (Li *et al* 2019). The increase in AVOCs, in contrast with the large emission decreases of SO_2 (since 2005) and NO_x (since 2011) in China, has been put forward as a potential reason for recent increases in surface ozone concentrations in China (Ma *et al* 2016, Li *et al* 2019).

5. Conclusion

We used OMI satellite observations from 2005 to 2019 to derive long-term trends in HCHO columns, corrected for climate variability, over 133 cities in Asia.

Significant positive trends were observed in 64 cities, and negative trends in only 13 cities. Although the general patterns of OMI column trends are consistent with the emission inventories, several important discrepancies were found. AVOC emissions appear to increase in Iran, in particular in Tehran, contradicting the decline found in CAMS. In India as well, the robust positive trend of OMI columns seems underestimated by CAMS. Strong positive HCHO trends are observed over the Middle East. Generally positive, but weaker trends are found in China. As Chinese VOC regulations were only recently implemented, HCHO trends between 2005 and 2018 do not yet validate these efforts. Nevertheless, the effect of AVOC regulations is clearly seen in two important megacities (Dongguan and Chengdu). Finally, over Japan and Taiwan, negative trends are found, demonstrating that air quality regulations targeting AVOC emissions are effective in these countries. In Japan in particular, those regulations appear even more effective than suggested by the CAMS inventory. The contrast between the observed evolution of NO_2 and HCHO columns over Asian cities illustrates well that emission controls targeting NO_x sources have little or no impact on AVOC emissions, in particular over China, as the major sources of NO_x and AVOC are markedly different, and as the AVOC and NO_x emission factors are affected differently by emission controls. Those important differences between HCHO and NO_2 trends highlight the importance of legislation targeting specifically VOC emissions to improve air quality. The limited number of initiatives to regulate AVOC emissions in many Asian countries is evidenced by the detected positive HCHO column trends compared to countries were policy measures have been in place for a longer time, or where they were recently introduced.

ORCID iDs

B Verreyken ⬤ https://orcid.org/0000-0002-5297-8524
T Stavrakou ⬤ https://orcid.org/0000-0002-2952-8306

References

Barkley M P et al 2013 Top-down isoprene emissions over tropical South America inferred from SCIAMACHY and OMI formaldehyde columns J. Geophys. Res. Atmos. **118** 6849–68

Barkley M P, González Abad G, Kurosu T P, Spurr R, Torbatian S and Lerot C 2017 OMI air-quality monitoring over the Middle East Atmos. Chem. Phys. **17** 4687–709

Bauwens M, Stavrakou T, Müller J-F, De Smedt I, van Roozendael M, Werf G R, Wiedinmyer C, Kaiser J W, Sindelarova K and Guenther A 2016 Nine years of global hydrocarbon emissions based on source inversion of OMI formaldehyde observations Atmos. Chem. Phys. **16** 10133–58

Bhave P and Kulkarni N 2015 Air pollution and control legislation in India J. Inst. Eng. India A **96** 259–65

Boersma K F et al 2018 Improving algorithms and uncertainty estimates for satellite NO_2 retrievals: results from the quality assurance for the essential climate variables (QA4ECV) project Atmos. Meas. Tech. **11** 6651–78

Boersma K F, Eskes H, Richter A, De Smedt I, Lorente A, Beirle S, van Geffen J, Peters E, van Roozendael M and Wagner T 2017 QA4ECV NO_2 tropospheric and stratospheric vertical column data from OMI (version 1.1) [data set] (Royal Netherlands Meteorological Institute (KNMI)) (https://doi.org/10.21944/qa4ecv-no2-omi-v1.1)

Botta E and Yamasaki S 2020 Policies, regulatory framework and enforcement for air quality management: the case of Japan Environment Working Papers No. 156 p 60

Bray C D, Battye W H and Aneja V P 2019 The role of biomass burning agricultural emissions in the Indo-Gangetic Plains on the air quality in New Delhi, India Atmos. Environ. **218** 116983

Calvert J G, Orlando J J, Stockwell W R and Wallington T J 2015 The Mechanisms of Reactions Influencing Atmospheric Ozone (New York: Oxford University Press)

Cao H et al 2018 Adjoint inversion of Chinese non-methane volatile organic compound emissions using space-based observations of formaldehyde and glyoxal Atmos. Chem. Phys. **18** 15017–46

Chaliyakunnel S, Millet D B and Chen X 2019 Constraining emissions of volatile organic compounds over the Indian subcontinent using space-based formaldehyde measurements J. Geophys. Res. **124** 10525–45

China VOCs management ChemLinked (available at: http://chemical.chemlinked.com/chempedia/china-volatile-organic-compounds-voc-s-management) (Accessed 26 July 2021)

Compernolle S et al 2020 Validation of Aura-OMI QA4ECV NO_2 climate data records with ground-based DOAS networks: the role of measurement and comparison uncertainties Atmos. Chem. Phys. **20** 8017–41

De Smedt I et al 2018 Algorithm theoretical baseline for formaldehyde retrievals from S5P TROPOMI and from the QA4ECV Project Atmos. Meas. Tech. **11** 2395–426

De Smedt I et al 2021 Comparative assessment of TROPOMI and OMI formaldehyde observations and validation against MAX-DOAS network column measurements Atmos. Chem. Phys. **21** 12561–93

Duncan B N, Lamsal L M, Thompson A M, Yoshida Y, Lu Z, Streets D G, Hurwitz M M and Pickering K E 2016 A space-based, high-resolution view of notable changes in urban NO_x pollution around the world (2005–2014) J. Geophys. Res. **121** 976–96

Ehhalt D et al 2001 Chapter 4, atmospheric chemistry and greenhouse gases Climate Change 2001: The Scientific Basis. Contribution of Working Group I to the Third Assessment Report of the Intergovernmental Panel on Climate Change ed J T Houghton et al (Cambridge: Cambridge University Press) p 50

Elguindi N et al 2020 Intercomparison of magnitudes and trends in anthropogenic surface emissions from bottom-up inventories, top-down estimates, and emission scenarios Earth's Future **8** e2020EF001520

EPA-Taiwan (Environmental Protection Administration) 2020 EPA control station Sources Air Pollut. 固定污染源管制 (available at: www.epa.gov.tw/eng/3C6700D26EC475B1) (Accessed 26 July 2021)

Ganguly T, Selvaraj K L and Guttikunda S K 2020 National Clean Air Programme (NCAP) for Indian cities: review and outlook for clean air action plans Atmos. Environ. **8** 100096

Gao H, Yang W, Wang J and Zheng X 2021 Analysis of the effectiveness of air pollution control policies based on historical evaluation and deep learning forecast: a case study of Chengdu-Chongqing region in China Sustainability **13** 206

Gao H, Yang W, Yang Y and Yuan G 2019 Analysis of the air quality and the effect of governance policies in China's Pearl River Delta, 2015–2018 Atmosphere **10** 412

Granier C et al 2019 The Copernicus atmosphere monitoring service global and regional emissions (April 2019 version) (https://doi.org/10.24380/d0bn-kx16)

Hansen M C et al 2013 High-resolution global maps of 21st-century forest cover change Science **342** 850–3

He Z, Wang X, Ling Z, Zhao J, Guo H, Shao M and Wang Z 2019 Contributions of different anthropogenic volatile organic compound sources to ozone formation at a receptor site in the Pearl River Delta region and its policy implications Atmos. Chem. Phys. **19** 8801–16

Hesbach H et al 2020 The ERA5 global reanalysis Q. J. R. Meteorol. Soc. **146** 1999–2049

Huang G, Brook R, Crippa M, Janssens-Maenhout G, Schieberle C, Dore C, Guizzardi D, Muntean M, Schaaf E and Friedrich R 2017 Speciation of anthropogenic emissions of non-methane volatile organic compounds: a global gridded data set for 1970–2012 Atmos. Chem. Phys. **17** 7683–701

Kurokawa J and Ohara T 2020 Long-term historical trends in air pollutant emissions in Asia: regional emission inventory in Asia (REAS) version 3 Atmos. Chem. Phys. **20** 12761–93

Levelt F L, van der Oord G H J, Dobber M R, Mälkki A, Visser H, de Vries J, Stammes P, Lundell J O V and Saari H 2006 The ozone monitoring instrument IEEE Trans. Geosci. Remote Sens. **44** 1093–101

Li M et al 2017 MIX: a mosaic Asian anthropogenic emission inventory under the international collaboration framework of the MICS-Asia and HTAP Atmos. Chem. Phys. **17** 935–63

Li M et al 2019 Persistent growth of anthropogenic non-methane volatile organic compound (NMVOC) emissions in China during 1990–2017: drivers, speciation and ozone formation potential Atmos. Chem. Phys. **19** 8897–913

Liu M, Song Y, Yao H, Kang Y, Li M, Huang X and Hu M 2015 Estimating emissions from agricultural fires in the North China Plain based on MODIS fire radiative power Atmos. Environ. **112** 326–34

Ma Z, Xu J, Quan W, Zhang Z, Lin W and Xu X 2016 Significant increase of surface ozone at a rural site, north of eastern China Atmos. Chem. Phys. **16** 3969–77

Marais E A, Jacob D J, Wecht K, Lerot C, Zhang L, Yu K, Kurosu T P, Chance K and Sauvage B 2014 Anthropogenic emissions in Nigeria and implications for atmospheric ozone pollution: a view from space Atmos. Environ. **99** 32–40

Millet D B, Jacob D J, Boersma K F, Fu T, Kurosu T P, Chance K, Heald C L and Guenther A 2008 Spatial distribution of isoprene emissions from North America derived from formaldehyde column measurements by the OMI satellite sensor J. Geophys. Res. **113** D02307

Müller J-F, Stavrakou T, Wallens S, De Smedt I, van Roozendael M, Potosnak M J, Rinne J, Munger B, Goldstein A and Guenther A B 2008 Global isoprene emissions estimated using MEGAN, ECMWF analyses and a detailed canopy environment model Atmos. Chem. Phys. **8** 1329–41

Nelson B S et al 2021 In situ ozone production is highly sensitive to volatile organic compounds in Delhi, India Atmos. Chem. Phys. **21** 13609–30

Opacka B, Müller J-F, Stavrakou T, Bauwens M, Sindelarova K, Markova J and Guenther A B 2021 Global and regional impacts of land cover changes on isoprene emissions derived from spaceborne data and the MEGAN model *Atmos. Chem. Phys.* **21** 8413–36

Palmer P I *et al* 2006 Quantifying the seasonal and interannual variability of North American isoprene emissions using satellite observations of the formaldehyde column *J. Geophys. Res.* **111** D12315

San V, Spoann V and Schmidt J 2018 Industrial pollution load assessment in Phnom Penh, Cambodia using an industrial pollution projection system *Sci. Total Environ.* **615** 990–9

Sekar A, Varghese G K and Ravi Varma M K 2019 Analysis of benzene air quality standards, monitoring methods and concentrations in indoor and outdoor environment *Heliyon* **5** e02918

Shen L *et al* 2019 The 2005–2016 trends of formaldehyde columns over china observed by satellites: increasing anthropogenic emissions of volatile organic compounds and decreasing agricultural fire emissions *Geophys. Res. Lett.* **46** 4468–75

Stavrakou T *et al* 2016 Substantial underestimation of post-harvest burning emissions in the North China Plain revealed by multi-species space observations *Sci. Rep.* **6** 32307

Stavrakou T, Müller J-F, Bauwens M and De Smedt I 2017 Sources and long-term trends of ozone precursors to Asian pollution *Air Pollution in Eastern Asia: An Integrated Perspective* ed I Bouarar, X Wang and G Brasseur (Cham: Springer International Publishing) pp 167–89

Stavrakou T, Müller J-F, Bauwens M, De Smedt I, van Roozendael M and Guenther A 2018 Impact of short-term climate variability on volatile organic compounds emissions assessed using OMI satellite formaldehyde observations *Geophys. Res. Lett.* **45** 8681–9

Stavrakou T, Müller J-F, De Smedt I, van Roozendael M, van der Werf G R, Giglio L and Guenther A 2009 Evaluating the performance of pyrogenic and biogenic emission inventories against one decade of space-based formaldehyde columns *Atmos. Chem. Phys.* **9** 1037–60

Tan Q, Zhou L, Liu H, Feng M, Qiu Y, Yang F, Jiang W and Wei F 2020 Observation-based summer O$_3$ control effect evaluation: a case study in Chengdu, a megacity in Sichuan Basin *China Atmos.* **11** 1278

Tsai W-T 2016 Toxic volatile organic compounds (VOCs) in the atmospheric environment: regulatory aspects and monitoring in Japan and Korea *Environments* **3** 23

United Nations Department of Economic and Social Affairs Population division 2018 world urbanization prospects: the 2018 revision (available at: https://population.un.org/wup/Download) (Accessed 30 September 2021)

Vohra K *et al* 2020 Long-term trends in air quality in major cities in the UK and India: a view from space *Atmos. Chem. Phys.* **21** 6275–96

Wakamatsu S, Morikawa T and Ito A 2013 Air pollution trends in Japan between 1970 and 2012 and impact of urban air pollution countermeasures *Asian J. Atmos. Environ.* **7** 177–90

Wang Y, Wang Z, Yu C, Zhu S, Cheng L, Zhang Y and Chen L 2019 Validation of OMI HCHO products using MAX-DOAS observations from 2010 to 2016 in Xianghe, Beijing: investigation of the effects of aerosols on satellite products *Remote Sens.* **11** 203

Zara M *et al* 2018 Improved slant column density retrieval of nitrogen dioxide and formaldehyde for OMI and GOME-2A from QA4ECV: intercomparison, uncertainty characterisation, and trends *Atmos. Meas. Tech.* **11** 4033–58

Zhao Q, Bi J, Liu Q, Ling Z, Shen G, Chen F, Qiao Y, Li C and Ma Z 2020 Sources of volatile organic compounds and policy implications for regional ozone pollution control in an urban location of Nanjing, East China *Atmos. Chem. Phys.* **20** 3905–19

Zheng B *et al* 2018 Trends in China's anthropogenic emissions since 2010 as the consequence of clean air actions *Atmos. Chem. Phys.* **18** 14095–111

Zhu L, Mickley L J, Jacob D J, Marais E A, Sheng J, Hu L, Abad G G and Chance K 2017 Long-term (2005–2014) trends in formaldehyde (HCHO) columns across North America as seen by the OMI satellite instrument: evidence of changing emissions of volatile organic compounds *Geophys. Res. Lett.* **44** 7079–86